

# EXPERIMENTS WITH AN ISOLATED SUBATOMIC PARTICLE AT REST

Nobel Lecture, December 8, 1989

by

HANS G. DEHMELT

Department of Physics, University of Washington, Seattle, WA 98195, USA

*"You know, it would be sufficient to really understand the electron."*

*Albert Einstein*

The 5th century B.C. philosopher's Democritus' smallest conceivable indivisible entity, the a-tomon (the un-cuttable), is a most powerful but not an immutable concept. By 1920 it had already metamorphosed twice: from something similar to a molecule, say a slippery atomon of water, to Mendeleev's chemist's atom and later to electron and to proton, both particles originally assumed to be of small but finite size. With the rise of Dirac's theory of the electron in the late twenties their size shrunk to mathematically zero. Everybody "knew" then that electron and proton were indivisible Dirac point particles with radius  $R = 0$  and gyromagnetic ratio  $g = 2.00$ . The first hint of cuttability or at least compositeness of the proton came from Stern's 1933 measurement of proton magnetism in a Stern-Gerlach molecular beam apparatus. However this was not realized at the time. He found for its normalized dimensionless gyromagnetic ratio not  $g = 2$  but

$$g = (\mu/A)(2M/q) \approx 5,$$

where  $\mu$ ,  $A$ ,  $M$ ,  $q$  are respectively magnetic moment, angular momentum, mass and charge of the particle. For comparison the obviously composite  ${}^4\text{He}^+$  ion, also with spin  $1/2$ , according to the above formula has the  $|g|$  value 14700, much larger than the Dirac value 2. Also, along with this large  $|g|$  value went a size of this atomic ion about 4 orders of magnitude larger than an  $\alpha$ -particle. And indeed, with Hofstadter's high energy electron scattering experiments in the fifties the proton radius grew again to  $R = 0.86 \times 10^{-15}$  m. Similar later work at still higher energies found 3 quarks inside the "indivisible" proton. Today everybody "knows" the *electron* is an indivisible atomon, a Dirac point particle with radius  $R = 0$  and  $g = 2.00$ .... But is it? Like the proton, it could be a composite object. History may well repeat itself. This puts a high premium on precise measurements of the  $g$  factor of the electron.

## GEONIUM SPECTROSCOPY

The metastable pseudo-atom geonium (Van Dyck et al. 1978 and 1986) has been expressly synthesized for studies of the electron  $g$  factor under optimal conditions. It consists of an individual electron permanently confined in an ultrahigh vacuum Penning trap at 4K. The trap employs a homogeneous magnetic field  $B_0 = 5\text{T}$  and a weak electric quadrupole field. The latter is produced by hyperbolic electrodes, a positive ring and two negative caps spaced  $2Z_0 = 8\text{ mm}$  apart, see Fig. 1. The potential, with  $A$  a constant, is given by

$$\phi(xyz) = A(x^2 + y^2 - 2z^2),$$

with an axial potential well depth

$$D = e[\phi(000) - \phi(00Z_0)] = 2eAZ_0^2 = 5\text{eV}.$$

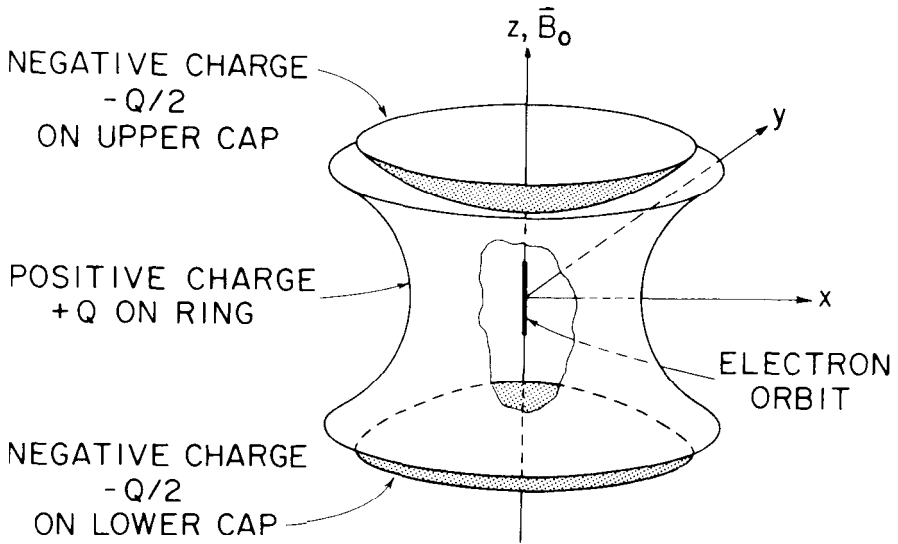


Figure 1. Penning trap. The simplest motion of an electron in the trap is along its symmetry axis, along a magnetic field line. Each time it comes too close to one of the negatively charged caps it turns around. The resulting harmonic oscillation took place at about 60 MHz in our trap. Reproduced from (Dehmelt 1983) with permission, copyright Plenum Press.

The trapping is mostly magnetic. The large magnetic field dominates the motion in the geonium atom. The energy levels of this atom shown in Figure 2 reflect the cyclotron motion, at frequency  $\nu_c = eB_0/2\pi m = 141\text{ GHz}$ , the spin precession, at  $\nu_s, -\nu_s$ , the anomaly or  $g-2$  frequency  $\nu_a = \nu_s - \nu_c = 164\text{ MHz}$ , the axial oscillation, at  $\nu_z = 60\text{ MHz}$ , and the magnetron or drift motion at frequency  $\nu_m = 13\text{ kHz}$ . The electron is continuously monitored by exciting the  $\nu_z$ -oscillation and detecting via radio the  $10^8$ -fold enhanced spontaneous 60 MHz emission. A corresponding signal appears in Figure 3.

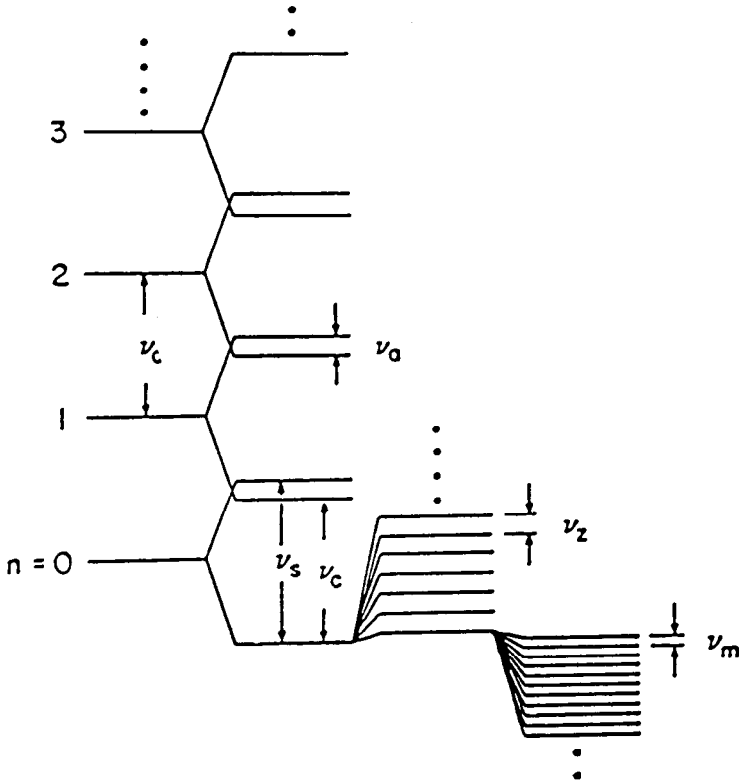


Figure 2. Energy levels of geonium. Each of the cyclotron levels labeled  $n$  is split first by the spin - magnetic field interaction. The resulting sublevels are further split into the oscillator levels and finally the manifold of magnetron levels extending downwards. Reproduced from (Van Dyck et al. 1978) with permission, copyright Plenum Press.

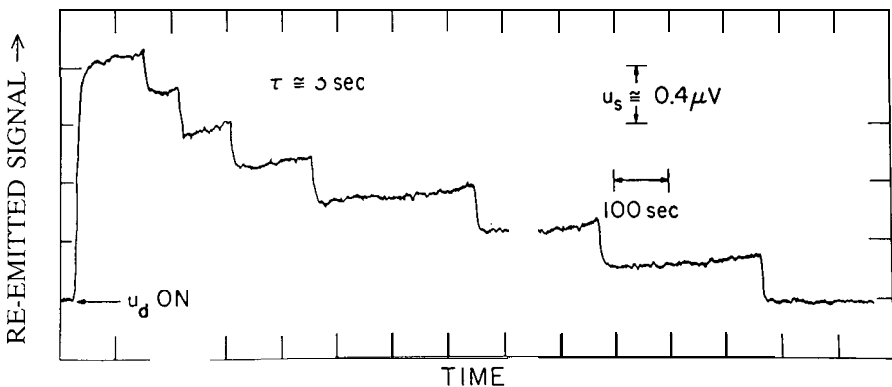


Figure 3. Rf signal produced by trapped electron. When the electron is driven by an axial rf field, it emits a 60 MHz signal, which was picked up by a radio receiver. The signal shown was for a very strong drive and an initially injected bunch of 7 electrons. One electron after the other was randomly "boiled" out of the trap until finally only a single one is left. By somewhat reducing the drive power, this last electron could be observed indefinitely. Reproduced from (Wineland et al. 1973) with permission, copyright American Institute of Physics.

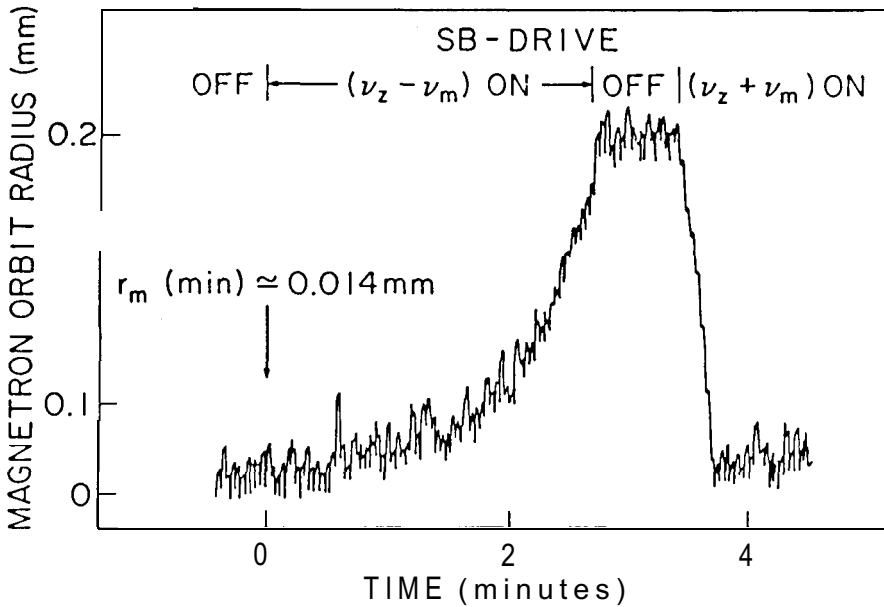


Figure 4. Side-band “cooling” of the magnetron motion at  $\nu_m$ . By driving the axial motion not on resonance at  $\nu_z$  but on the lower side-band at  $\nu_z - \nu_m$  it is possible to force the metastable magnetron motion to provide the energy balance  $h\nu_m$ , and thereby expand the magnetron orbit radius. Conversely, an axial drive at  $\nu_z + \nu_m$  shrinks the radius. The roles of upper and lower side-bands are reversed here from the case of a particle in a well where the energy increases with amplitude because the magnetron motion is metastable and the total energy of this motion decreases with radius. Reproduced from (Van Dyck et al. 1978) with permission, copyright Plenum Press.

Side band cooling has made continuous confinement in the trap center of an electron for 10 months (Gabrielse et al. 1985) possible. This process makes the electron absorb rf photons deficient in energy and supply the balance from energy stored in the electron motion to be cooled. The corresponding shrinking of the radius of the magnetron motion is displayed in Figure 4. Extended into the optical region, the cooling scheme is most convincingly demonstrated in Figure 5. The transitions of primary interest at  $\nu_c$ ,  $\nu_a$ ,  $\nu_m$  are much more difficult to detect than the  $\nu_z$  oscillation. Nevertheless the task may be accomplished by means of the continuous Stern-Gerlach effect (Dehmelt 1988a), in which the geonium atom itself is made to work as a  $10^8$ -fold amplifier. In the scheme a single  $\nu_a$ -photon of only  $\approx 1\mu\text{eV}$  energy gates the absorption of  $\approx 100\text{ eV}$  of rf power at  $\nu_c$ . The continuous effect uses an inhomogeneous magnetic field in a similar way as the classic one. However, the field takes now the form of a very weak Lawrence cyclotron trap or magnetic bottle shown in Figure 6. The bottle adds a minute monitoring well, only

$$D_m = (m + n + 1/2) 0.1\mu\text{eV}$$

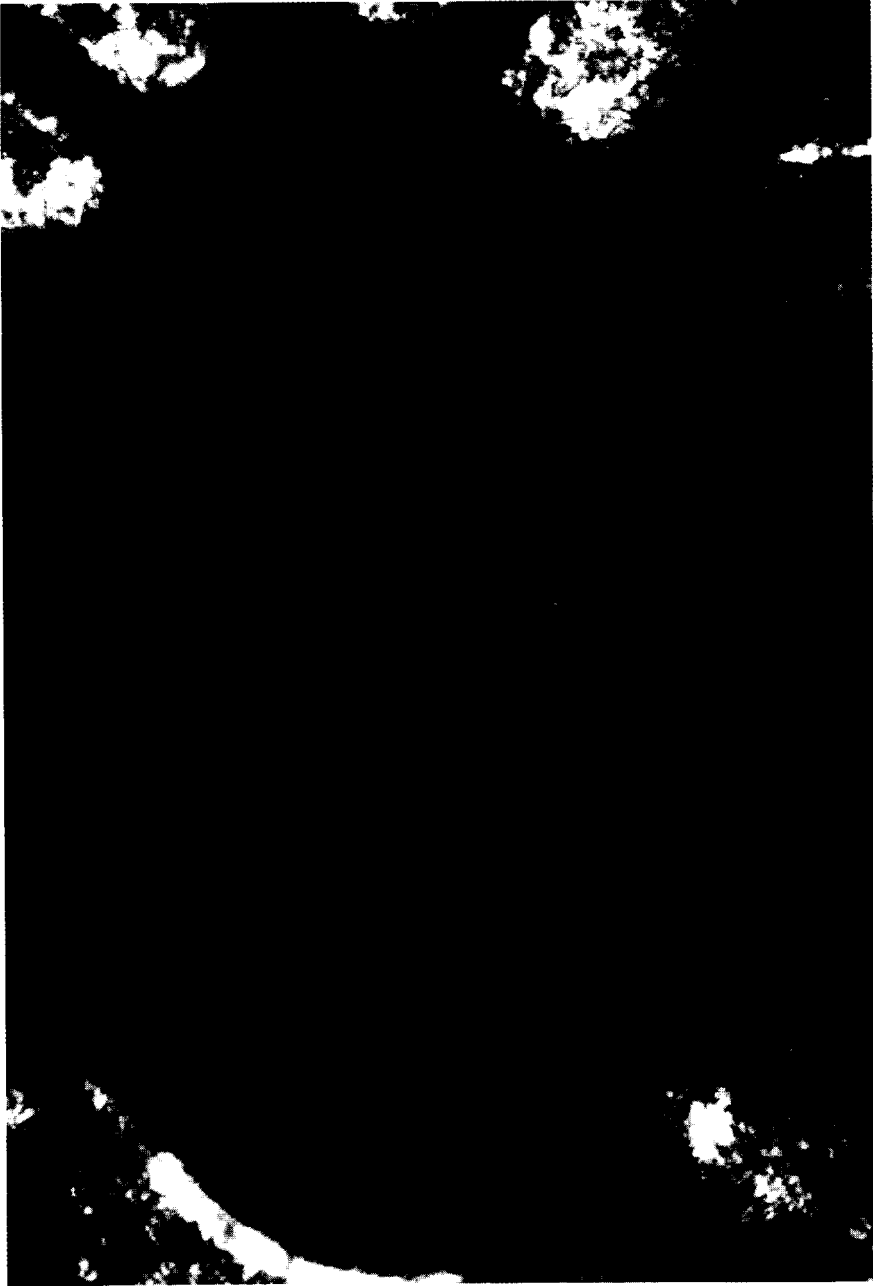


Figure 5. Visible blue (charged) barium atom Astrid at rest in center of Paul trap photographed in natural color. The photograph strikingly demonstrates the close localization,  $< 1 \mu\text{m}$ , attainable with geonium techniques. Stray light from the lasers focussed on the ion also illuminate the ring electrode of the tiny rf trap of about 1 mm internal diameter. Reproduced from (Dehmelt 1988) with permission, copyright the Royal Swedish Academy of Sciences.

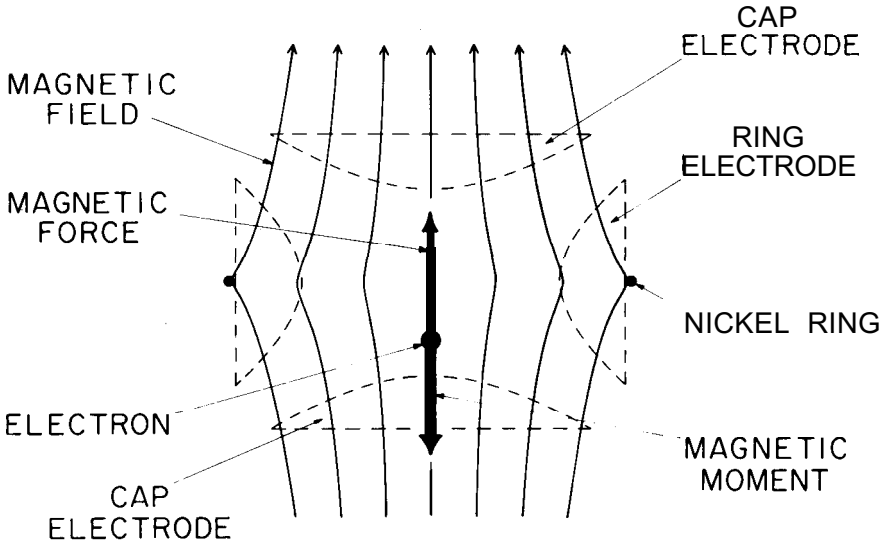


Figure 6. Weak magnetic bottle for continuous Stern-Gerlach effect. When in the lowest cyclotron and magnetron level the electron forms a 1  $\mu\text{m}$  long wave packet, 30 nm in diameter, which may oscillate undistorted in the axial electric potential well. The inhomogeneous field of the auxiliary magnetic bottle produces a minute spin-dependent restoring force that causes the axial frequency  $\nu_z$  for spin  $\uparrow$  and  $\downarrow$  to differ by a small but detectable value. Reproduced from (Dehmelt 1988a) with permission, copyright Springer Verlag.

deep, to the axial well of large electrostatic depth  $D = 5\text{eV}$ , with  $m, n$  respectively denoting spin and cyclotron quantum numbers. Thus jumps in  $m$  or  $n$  show up as jumps in  $\nu_z$

$$\nu_z = \nu_{z0} + (m + n + 1/2)\delta,$$

with  $\delta = 1.2\text{Hz}$  in our experiments, and  $\nu_{z0}$  the axial frequency of a hypothetical electron without magnetic moment. Random jumps in  $m, n$  occur, when spin or cyclotron resonances are excited. Figure 6A shows an early example of a series of such jumps in  $m$  or spin flips. For the spin spontaneous transitions are totally negligible. Standard text books discuss

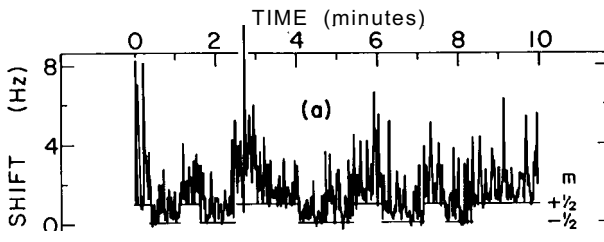


Figure 6A. Spin flips recorded by means of the continuous Stern-Gerlach effect. The random jumps in the base line indicate jumps in  $m$  at a rate of about 1/minute when the spin resonance is excited. The upwards spikes or “cyclotron grass” are explained by expected rapid random thermal excitation and spontaneous decay of cyclotron levels with an average value  $\langle n \rangle \approx 1.2$ . Adapted from (Van Dyck et al. 1977) with permission, copyright American Institute of Physics.

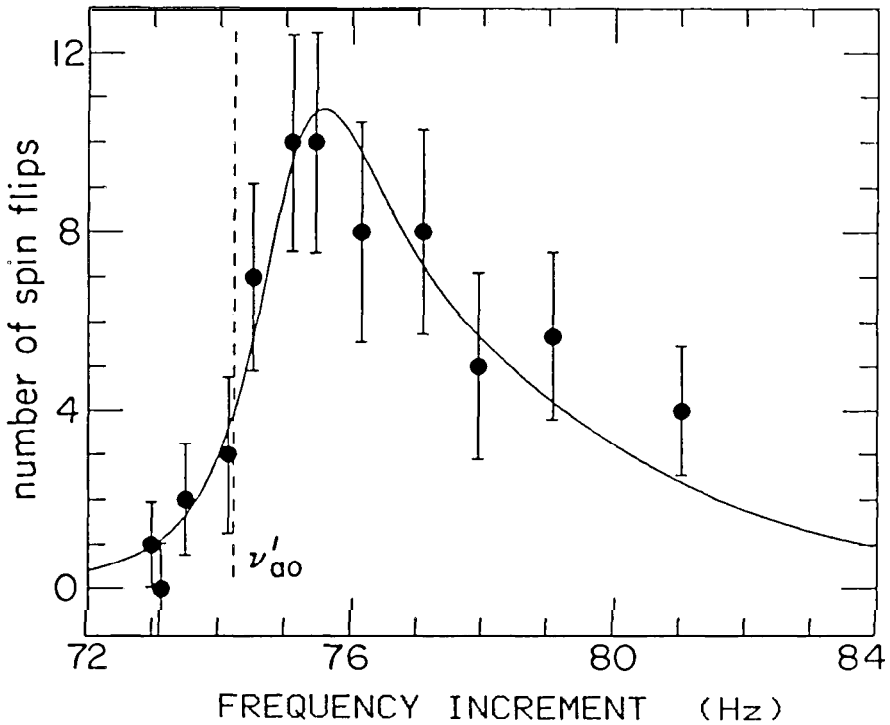


Figure 7. Plot of electron spin resonance in geonium near 141 GHz. A magnetic radiofrequency field causes random jumps in the spin quantum number. As the frequency of the exciting field is stepped through the resonance in small increments, the number of spin flips occurring in a fixed observation period of about  $\frac{1}{2}$  hour are counted and then plotted vs frequency. (Actually the 141 GHz field flipping the spin is produced by the cyclotron motion of the electron through an inhomogeneous magnetic rf field at  $\nu_c - \nu_e = 164$  MHz.) Reproduced from (Van Dyck et al. 1987) with permission, copyright American Institute of Physics.

transitions between two sharp levels induced by a broad electromagnetic spectrum  $\rho(\nu)$ : The transition rate from either level is the same and is proportional to the spectral power density  $\rho(\nu_s)$  of the radiation field at the transition frequency  $\nu_s$ . Ergo, the average dwell times in either level are the same, compare Fig. 6A. In the geonium experiments the frequency of the weak rf field is sharp, but the spin resonance is broadened and has a shape  $G_s(\nu)$ . One may convince oneself that moving the sharp frequency of the rf field upwards over the broad spin resonance should produce the same results as moving a broad rf field of spectral shape  $\rho(\nu) \propto G_s(\nu)$  downwards over a sharp spin resonance: The rate of all spin flips or jumps in  $m$  in either direction counted in the experiment is proportional to  $G_s(\nu)$ . To obtain the plot of  $G_s(\nu)$  in Fig. 7 the frequency of the rf field was increased in small steps, and at each step spin flips were counted for a fixed period of about  $\frac{1}{2}$  hour. From our  $\nu_e, \nu_c$  data for electron and positron (Van Dyck et al. 1987) we have determined

$$\frac{1}{2}g^{\text{exp}} = \nu_s/\nu_c = 1.001\,159\,652\,188(4),$$

the same for particle and anti-particle. The error in their difference is only half as large. Heroic quantum electro-dynamical calculations (Kinoshita 1988) have now yielded for the shift of the  $g$  factor of a point electron associated with turning on its interaction with the electromagnetic radiation field

$$\frac{1}{2}(g^{\text{point}} - 2) = \frac{1}{2}\Delta g^{\text{KINOSHITA}} = 0.001\ 159\ 652\ 133(29).$$

In the calculations  $\Delta g^{\text{KINOSHITA}}$  is expressed as a power series in  $\alpha/\pi$ . Kinoshita has critically evaluated the experimental input data on which he must rely. He warns that the error in his above result, which is dominated by the error in  $a$ , may be underestimated. Muonic, hadronic and other small contributions to  $g$  amount to less than about  $4 \times 10^{-12}$  and have been included in the shift. Kinoshita's result may be used to correct the experimental  $g$  value and find

$$g = g^{\text{exp}} - \Delta g^{\text{KINOSHITA}} = 2 + 11(6) \times 10^{-11}.$$

ELECTRON RADIUS R?

Extrapolation from known to unknown phenomena is a time-honored approach in all the sciences. Thus from known  $g$ , and  $R$  values of other near-Dirac particles and our *measured*  $g$  value of the electron I attempt to extrapolate a value for its radius. Stimulated by 1980 theoretical work of Brodsky & Drell, I (1989a) have plotted  $|g-2| = R/\lambda_c$  in Figure 8 for the helium3 nucleus, triton, proton, and electron. Here  $\lambda_c$  is the Compton wavelength of the respective particle. The plausible relation given by Brodsky and Drell (1980) for the simplest composite theoretical model of the electron,

$$|g - 2| = R/\lambda_c, \text{ or}$$

$$|g - g_{\text{DIRAC}}| = R/\lambda_c$$

fits the admittedly sparse data surprisingly well. Even for such a very different spin  $1/2$  structure as the atomic ion  ${}^4\text{He}^+$  composed of an  $\alpha$ -particle and an electron the data point does not fall too far off the full line. Intersection in Figure 8 of this line with the line  $|g-2| = 1.1 \times 10^{-10}$  for the Seattle  $g$  data yields for the electron the extrapolated point shown and with  $\lambda_c = 0.39 \times 10^{-10}$  cm an electron radius

$$R \approx 10^{-20} \text{ cm.}$$

The row of X's reflects the data range defined by the uncertainty in the Seattle  $g$  data and the upper limit  $R < 10^{-17}$  cm determined in high energy collision experiments. It appears that this combination of current data is not in harmony with electron structure models assuming special symmetries that predict the quadratic relation  $|g-2| \approx (R/\lambda_c)^2$  shown by the dashed line. This favors the linear relation used in the above extrapolation of  $R$  for the electron. Thus, the electron may have *size and structure!*

If one feels that the excess  $g$  value  $11(6) \times 10^{-11}$  measured is not signifi-



## NEAR-DIRAC PARTICLE DATA

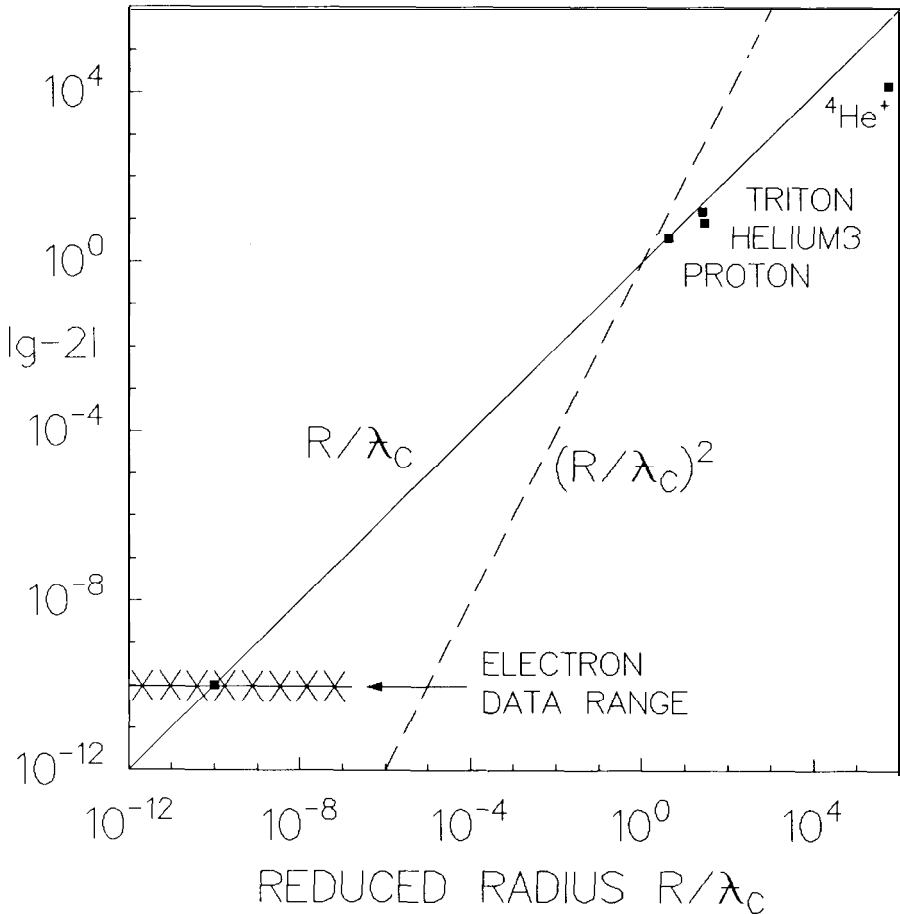


Figure 8. Plot of  $|g-2|$  values, with radiative shifts removed, vs reduced rms radius  $R/\lambda_c$  for near-Dirac particles. The full line ( $g-2l = R/\lambda_c$ , predicted by the simplest theoretical model provides a surprisingly good fit to the data points for proton, triton and helium3 nucleus. It may be used to obtain a new radius value for the *physical* electron from its intersection with the line  $|g-2| = 1.1 \times 10^{-10}$  representing the Seattle electron  $g$  data. The data are much less well fitted by the relation  $|g-2| = (R/\lambda_c)^2$ , which is shown for comparison in the dashed line. The atomic ion  ${}^4\text{He}^+$  is definitely *not* a near-Dirac particle, but even its data point does not fall too far off the full line. Adapted from (Dehmelt 1990) with permission, copyright American Institute of Physics.

cant because of its large relative error then, the value  $R \approx 10^{-20}$  cm given here still constitutes an important new upper limit. Changing the point of view, the close agreement of  $g^{\text{point}}$  with  $g^{\text{exp}}$  provides the most stringent experimental test of the fundamental theory of Quantum Electrodynamics in which  $R = 0$  is assumed. Furthermore the near-identity of the  $g$  values measured for electron and positron in Seattle constitutes the most severe test of the CPT theorem or mirror symmetry of a *charged* particle pair.

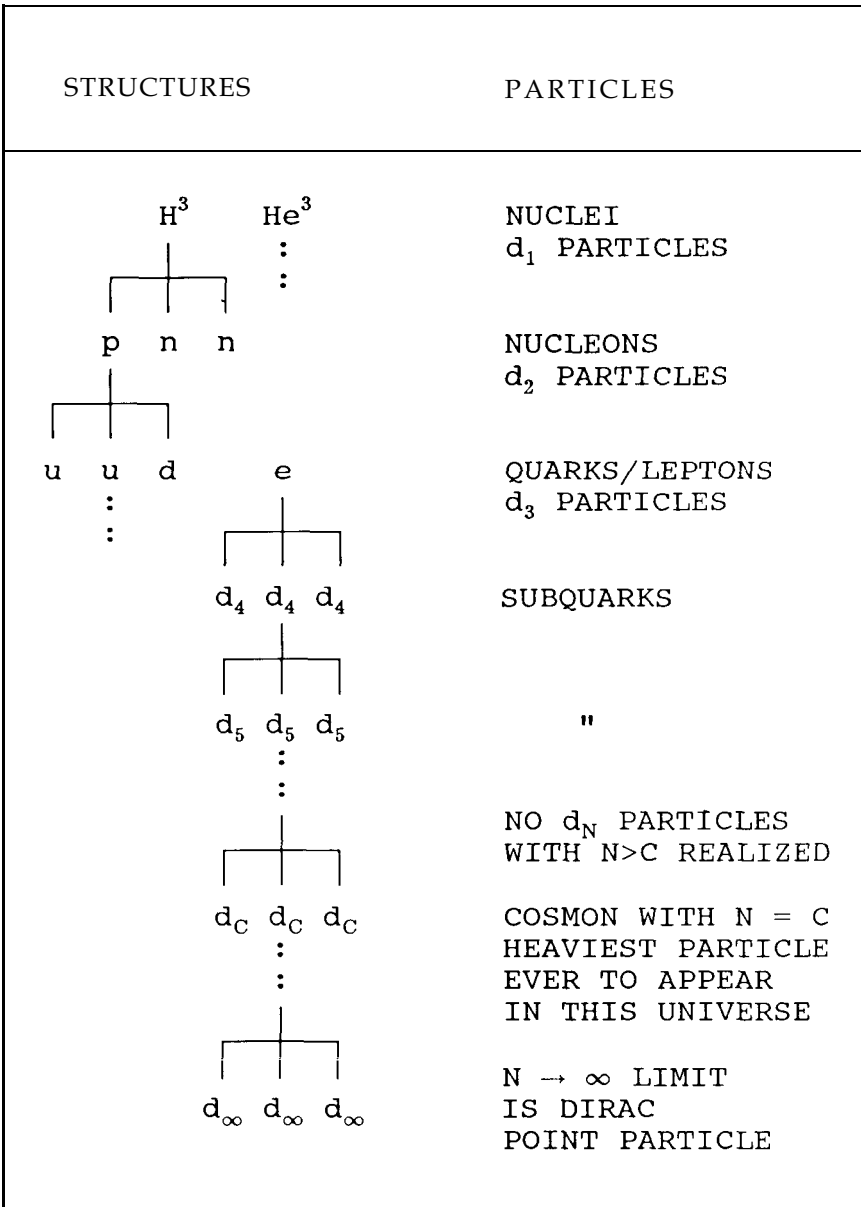


Figure 9. Triton model of near-Dirac particles. Reproduced from (Dehmelt 1989b) with permission, copyright the National Academy of Sciences of the USA.

LEMAÎTRE'S "L'ATOME PRIMITIF" REVISITED - A SPECULATION  
 Beginning 1974 Salam and others have proposed composite electron and quark models (Lyons 1983). On the strength of these proposals and with an eye on Figure 8, I view the electron as the third approximation of a Dirac particle,  $d_3$  for short, and as composed of three fourth-approximation Dirac

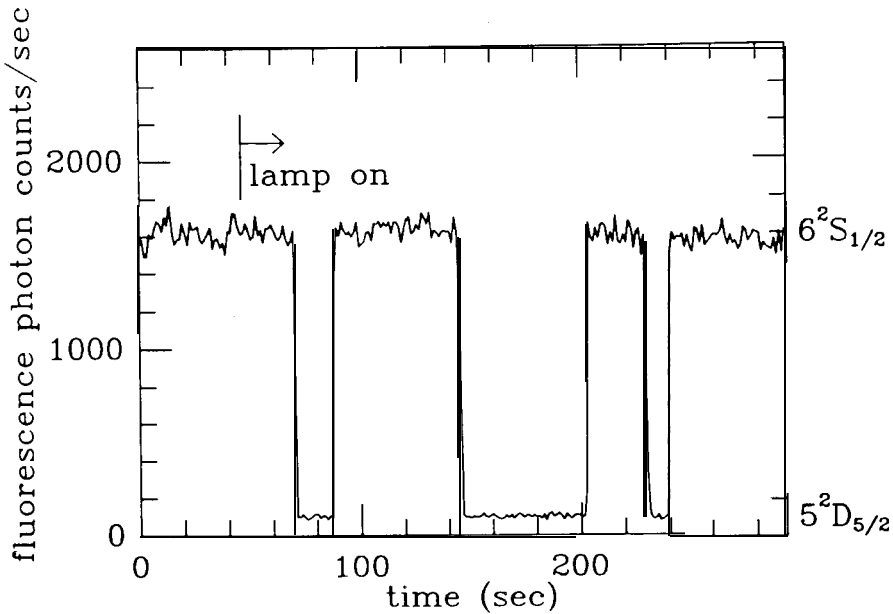


Figure 10. Spontaneous decay of  $\text{Ba}^+$  ion in metastable  $D_{5/2}$ -level. Illuminating the ion with a laser turned close to its resonance line produces strong resonance fluorescence and an easily detectable photon count of 1600 photons/sec. When later an auxiliary, weak  $\text{Ba}^+$  spectral lamp is turned on the ion is randomly transported into the metastable  $D_{5/2}$  level of 30 sec lifetime and becomes invisible. After dwelling in this shelving level for 30 sec on the average, it drops down to the  $S_{1/2}$  ground state *spontaneously* and becomes visible again. This cycle then repeats. Reproduced from (Nagourney et al. 1986) with permission, copyright American Institute of Physics.

or  $d_4$  particles. The situation is taken to be quite similar to that previously encountered in the triton and proton subatomic particles, respectively assumed to be of type  $d_1$  and  $d_2$ . In more detail, three  $d_4$  subquarks of huge mass  $m_4$  in a deep square well make up the electron in this working hypothesis. However, their mass  $3m_4$  is almost completely compensated by strong binding to yield a total relativistic mass equal to the observed mass  $m_e$  of the electron. Figure 8 may even suggest a more speculative extrapolation: The  $e$ -constituents, in the infinite regression  $N \rightarrow \infty$  - proposed in Figure 9, have ever more massive, ever smaller sub-sub-... constituents  $d_N$ . However, these higher order subquarks are realized only up to the "cosmon" with  $N = C$ , the most massive particle ever to appear in this universe. At the beginning of the universe, a lone bound cosmon-anticosmon pair or life time-broadened cosmonium atom state of near-zero total relativistic mass/energy was created from Vilenkin's (1984) metastable "nothing" state of zero relativistic energy in a spontaneous quantum jump of cosmic rarity. Similar, though much more frequent, quantum jumps that have recently been observed in a trapped  $\text{Ba}^+$  ion are shown in Figure 10. In this case the system also jumps spontaneously from a state (ion in metastable  $D_{5/2}$  level

plus no photon) to a new state (ion in  $S_{\frac{1}{2}}$  ground level plus photon) of the same total energy. The "cosmonium atom" introduced here is merely a modernized version\* of Lemaître's "l'atome primitif" or world-atom whose explosive radioactive decay created the universe. At the beginning of the world the short-lived cosmonium atom decayed into an early gravitation-dominated standard big bang state that eventually developed into a state, in which again rest mass energy, kinetic and Newtonian gravitational potential energy add up to *zero* (see formula 8 of Jordan 1937). The electron is a much more complex particle than the cosmon. It is composed of  $3^{c-3}$  cosmon-like  $d_c$ 's, but only two particles of this type formed the cosmonium world-atom from which sprang the universe. In closing, I should like to cite a line from *William Blake*.

*"To see a world in a grain of sand - - -"*

and allude to a possible parallel

to see worlds in an electron -

\* This is by no means the first modernization attempt. M. Goldhaber has kindly brought it to my attention that he had introduced a different "cosmon" already in 1956 in his paper "Speculations on Cosmogony," SCIENCE 124, 218.

## REFERENCES

- Brodsky, S. J., and Drell, S. D., "Anomalous Magnetic Moment and Limits on Fermion Substructure," *Phys. Rev. D* **22**, 2236 (1980).
- Dehmelt, H. (1983) "Stored Ion Spectroscopy", in *Advances in Laser Spectroscopy*, F. T. Arecchi, F. Strumia & H. Walther, Eds., Plenum, New York.
- Dehmelt, H. (1988a) "Single Atomic Particle Forever Floating at Rest in Free Space: New Value for Electron Radius," *Physica Scripta* **T22**, 102.
- Dehmelt, H. (1988b) "New Continuous Stern Gerlach Effect and a Hint of 'The' Elementary Particle," *Z. Phys. D* **10**, 127- 134.
- Dehmelt, H. (1989a) "Geonium Spectra \* Electron Radius \* Cosmon" in *High Energy Spin Physics*, 8th International Symposium, K. Heller, Ed. (AIP Conference Proceedings No. 187, New York) p. 319.
- Dehmelt, H. (1989b) "Triton,..electron,..cosmon..: An infinite regression?," *Proc. Natl. Acad. Sci. USA* **86**, 8618-8619.
- Dehmelt, H. (1990) "Less is more: Experiments with an Individual Atomic Particle at Rest in Free Space" *Am. J. Phys.*, **58**, 17.
- Gabrielse, G., Dehmelt, H., and Kells, W. (1985) "Observation of a Relativistic, Bistable Hysteresis in the Cyclotron Motion of a Single electron" *Phys. Rev. Letters* **54**, 537.
- Jordan, P., (1937) "Die physikalischen Weltkonstanten" *Naturwissenschaften* **25**, 513.
- Kinoshita, T. (1988) "Fine-Structure Constant Derived from Quantum Electrodynamics," *Metrologia* **25**, 233.
- Lemaître, G. (1950) *THE PRIMEVAL ATOM* (Van Nostrand, New York) p. 77.
- Lyons, L. (1983) "An Introduction to the Possible Substructure of Quarks and Leptons," *Progress in Particle and Nuclear Physics* **10**, 227, see references cited herein.
- Nagourney, W., Sandberg, J., and Dehmelt, H. (1986) "Shelved optical electron amplifier: Observation of quantum jumps." *Phys. Rev. Letters* **56**, 2797.
- Van Dyck, Jr., R. S., Ekstrom, P., and Dehmelt, H. (1977) "Precise Measurement of Axial, Magnetron, and Spin-Cyclotron Beat Frequencies on an Isolated 1-meV Electron", *Phys. Rev. Lett.* **38**, 310
- Van Dyck, Jr., R. S., Schwinberg, P. B. & Dehmelt, H. G. (1978) "Electron Magnetic Moment from Geonium Spectra," in *New Frontiers in High Energy Physics* (Eds. B. Kursunoglu, A. Perlmutter, and L. Scott), Plenum New York.
- Van Dyck, Jr., R. S., Schwinberg, P. B. & Dehmelt, H. G. (1986) "Electron Magnetic Moment from Geonium Spectra: Early Experiments and Background Concepts," *Phys. Rev. D* **34**, 722.
- Van Dyck, Jr., R. S., Schwinberg, P. B. & Dehmelt, H. G. (1987) "New High Precision Comparison of Electron/Positron g-Factors," *Phys. Rev. Letters* **59**, 26.
- Vilenkin, A. (1984) "Quantum Creation of Universe," *Phys. Rev. D* **30**, 509 - 5 15.
- Wineland, D., Ekstrom, P., and Dehmelt, H. (1973) "Monoelectron Oscillator," *Phys. Rev. Lett.* **31**, 1297.